PSFC/JA-08-39

Zonal flow in a tokamak pedestal

Grigory Kagan and Peter Catto

December 2008

Plasma Science and Fusion Center
Massachusetts Institute of Technology
Cambridge MA 02139 USA

This work was supported by the U.S. Department of Energy, Grant No. DE-FG02-91ER-54109 .

Submitted for publication in the Physics of Plasma (November 2008)

Zonal flow in a tokamak pedestal

Grigory Kagan and Peter J. Catto

Plasma Science and Fusion Center, MIT, Cambridge, MA, 02139, USA

E-mail: gkagan@mit.edu and catto@psfc.mit.edu

Neoclassical shielding is the dominant mechanism reducing the collisionless zonal flow in a tokamak. Previously, this phenomenon was analyzed in the case of an essentially homogeneous equilibrium since the wavelength of the zonal flow perturbation was assumed to be much less than the scale length of background plasma parameters. This assumption is not appropriate in a tokamak pedestal. Therefore the pedestal neoclassical polarization and the zonal flow residual differ from the conventional results. This change is due to the strong electric field intrinsic to a subsonic pedestal that modifies neoclassical ion orbits so that their response to a zonal flow perturbation is qualitatively different from that in the core. In addition to orbit squeezing, we find a spatial phase shift between the initial and final zonal flow potentials – an effect absent in previous works. Moreover, we demonstrate that because of orbit modification neoclassical phenomena disappear in the large electric field limit making the residual close to one.

I. INTRODUCTION

Zonal flow is observed in nearly all the systems with turbulent behavior[1]. In tokamaks, zonal flow is a poloidally and toroidally symmetric sheared flow produced by drift wave turbulence on a time scale greater than the cyclotron period. By suppressing this turbulence, it limits anomalous transport and in turn improves plasma confinement. This mechanism seems to be rather universal and works for turbulence due to ion[2-4] and electron[5] temperature gradient modes. In this connection, the question of what limits zonal flow itself takes on special significance.

The pioneering work by Rosenbluth and Hinton[6] demonstrated that in the absence of collisions the zonal flow amplitude is controlled by neoclassical polarization, with a significant portion of it, the residual, surviving in the turbulent steady state. In their calculation, the assumptions of circular flux surfaces and large radial wavelengths were used. In subsequent work the effects of collisions on zonal flow were analyzed[7, 8] as well as those of the flux surfaces shape[9, 10] and shorter wavelengths[11, 12]. However, all of the preceding analyses involved an essentially homogeneous equilibrium solution since the wavelength of the zonal flow perturbation was assumed to be much less than all background radial scale lengths. While plausible in the tokamak core, such an assumption is inappropriate in a pedestal whose background scale is comparable to the ion poloidal gyroradius $\rho_{pol} \equiv v_i Mc \,/\, ZeB_{pol}$, where $v_i \equiv \left(2T_i \,/\, M\right)^{1/2}$ is the ion thermal velocity and B_{pol} is the poloidal magnetic field. The purpose of the present calculation is to generalize the zonal flow calculation to the pedestal case.

A better understanding of the pedestal region is a key to modeling high confinement or H Mode operation[13, 14] for controlled fusion power production. Recently, some basic features inherent in a pedestal were theoretically found in Ref.[15]. The formalism developed there allows the radial pedestal

width to be of the order of ion poloidal gyroradius while assuming $\rho \ll \rho_{pol}$, where ρ is the ion gyroradius. This assumption decouples the neoclassical phenomena from classical finite Larmor radius (FLR) effects and allows the development of a version of gyrokinetics that is particularly convenient for pedestal studies. With the help of this formalism we proved that in the banana regime the background ion temperature in pedestal cannot vary as strongly as on the poloidal gyroradius scale when plasma density does. This result was recently confirmed by direct measurements in He plasmas in DIII-D[16]. Moreover, it allows the shape of the pedestal electric field to be deduced for subsonic ion flow since the $\vec{E} \times \vec{B}$ drift and diamagnetic flow must cancel to lowest order in ρ / ρ_{pol}.

When the pedestal width is of order ρ_{pol} it is important to recall that ion departures from a flux surface also scale with ρ_{pol} and therefore finite drift orbit effects on zonal flow are significant. For the problem of ion transport these effects were considered by Shaing and Hazeltine[17], who presented the derivation of ion orbits in the presence of a strongly sheared radial electric field. They focused their studies on orbit squeezing[18] by assuming large electric field shear and expanding the potential around the flux surface where the radial electric field vanished. However, the electric field is large for most flux surfaces in the pedestal and we are led to solve for the particle motion in a tokamak retaining both the electric field and its shear. A preliminary numerical investigation of this issue along with some analytical estimates is given in Ref.[19]. Here we present a fully self-consistent derivation of particle trajectories in a pedestal.

To carry out the pedestal zonal flow calculation we employ the Kagan and Catto[15] version of gyrokinetics that readily provides the relation between the density and potential perturbations. The explicit evaluation of the potential involves trajectory integrals and this is where the finite orbit

effects enter. We find that for strong enough electric field the trapped particle fraction becomes exponentially small so that the neoclassical shielding disappears. This means that turbulent transport can be lower in the pedestal than in the core for the same turbulent drive, and may impact for how a sharp density gradient is established on the transport time scale.

The remainder of the paper is organized as follows. In Sec. II we derive the integral relation between the density and potential perturbations and give the expression for the zonal flow residual. Sec. III investigates ion motion in a tokamak pedestal and the results of this study are applied in Sec. IV to obtain explicit expressions for the neoclassical polarization and the zonal flow residual in the pedestal. Finally, in Sec. V we summarize our findings and discuss their implications.

II. NEOCLASSICAL POLARIZATION IN THE PRESENCE OF STRONG BACKGROUND ELECTRIC FIELD

Rosenbluth and Hinton demonstrated that neoclassical polarization is the key factor affecting the zonal flow dynamics in a tokamak[6, 7]. Thus, to see how zonal flow is modified as we move from the tokamak core to the pedestal, we have to evaluate neoclassical polarization in the presence of a sharp density gradient.

It may seem that as polarization density is due to modifying single particle orbits by the perturbation of the electric field, the density gradient should not have a strong impact on it. However, while a density gradient cannot affect single particle motion directly, it necessarily builds up a strong electric field to sustain pressure balance[15, 20]. In a subsonic pedestal with a density gradient as large

as $1/\rho_{pol}$, the resulting $\vec{E}\times\vec{B}$ drift ($\vec{v}_E$) contributes to the poloidal angular velocity $\dot{\theta}$ of ions in leading order so that

$$\dot{\theta} = v_{\|}\hat{n}\cdot\nabla\theta + \vec{v}_E\cdot\nabla\theta = \left[v_{\|} + cI\phi'\left(\psi\right)/B\right]\hat{n}\cdot\nabla\theta\,, \tag{1}$$

where the two terms on the right side are comparable (unlike the core where $v_{\|}$ dominates). Therefore, the distinctive pedestal feature that is crucial for the zonal flow dynamics is the existence of the strong background radial electric field as it directly affects equilibrium particle orbits. Accordingly, in this section we discuss the role of the equilibrium electric field on the neoclassical plasma polarization.

Plasma polarization ε^{pol} relates density and potential perturbations δn and $\delta\phi$ through

$$\varepsilon^{pol}k_{\perp}^2\delta\phi = -4\pi Ze\delta n\,. \tag{2}$$

Therefore, what one technically has to do to evaluate ε^{pol} is to assume a small density perturbation is introduced into the pedestal and find the potential response to this perturbation. To this end, it is convenient to use the axisymmetric gyrokinetic equation derived in Ref.[15]

$$\frac{\partial g}{\partial t} - \overline{C_{ii}^l\left\{g - \frac{Iv_{\|}}{\Omega}f_M\frac{Mv^2}{2T^2}\frac{\partial T}{\partial\psi}\right\}} = -\frac{Ze}{M}\frac{\partial\langle\phi\rangle}{\partial t}\frac{\partial f_M}{\partial E}\,, \tag{3}$$

where instead of the regular radial variable we employ the canonical angular momentum

$$\psi_* \equiv \psi - \frac{Mc}{Ze}R\hat{\zeta}\cdot\vec{v} = \psi - \frac{Iv_{\|}}{\Omega} + \frac{\vec{v}\times\hat{n}}{\Omega}\cdot\nabla\psi \tag{4}$$

with I defining the toroidal component of the axisymmetric magnetic field $\vec{B} = I\nabla\zeta + \nabla\zeta\times\nabla\psi$ and $g \equiv f - f_M$, where f is the total ion distribution function. The other independent variables are the total energy $E \equiv v^2/2 + (Ze/M)\phi$, the poloidal and toroidal coordinates of the gyrocenter $\theta_* = \theta + \vec{v}\times\hat{n}\cdot\nabla\theta/\Omega$ and $\zeta_* = \zeta + \vec{v}\times\hat{n}\cdot\nabla\zeta/\Omega$, and magnetic moment μ. Here, gyroaveraging, denoted by $\left\langle ...\right\rangle$, is to be performed holding ψ_*, θ_*, ζ_*, E, and μ fixed, and C_{ii}^l

stands for the linearized ion-ion collision operator. Finally, to derive (3) the leading order solution is taken to be a Maxwellian whose temperature varies slowly on the poloidal gyroradius scale

$$f_M = \eta\left(\frac{M}{2\pi T}\right)^{3/2}\exp\left(-\frac{E}{T}\right) \tag{5}$$

with $\eta = n\exp\left(Ze\phi\ /\ T\right) \approx const$. It was proven analytically in Ref.[15] that in the banana regime this is the only physically acceptable choice giving no entropy production in the pedestal. This result is also confirmed experimentally by recent measurements in the DIII-D tokamak that found He ion temperature variation much slower than that of the density and electron temperature[16].

To apply (3) to our problem we have to evaluate $\langle\phi\rangle$. To do so we observe that there is a significant equilibrium potential in the pedestal and therefore ϕ consists of the unperturbed piece ϕ_0, whose gradient balances the diamagnetic drift to keep the ion flow subsonic [$\partial\phi_0\ /\ \partial\psi \approx -\left(T_i\ /\ en\right)\partial n\ /\ \partial\psi$], and the perturbation $\delta\phi$ such that $\partial\langle\phi\rangle/\partial t = \partial\langle\delta\phi\rangle/\partial t$. Assuming an eikonal form for $\delta\phi$ we write

$$\delta\phi = \hat{\phi}e^{iG(\psi)} \approx \hat{\phi}e^{iG\left(\psi_* + Iv_{||}/\Omega - \vec{v}\times\hat{n}\cdot\nabla\psi/\Omega\right)}. \tag{6}$$

Normally, we would expand G around ψ_* to obtain

$$G(\psi) \approx G\left(\psi_*\right) + \left(Iv_{||}/\Omega - \vec{v}\times\hat{n}\cdot\nabla\psi/\Omega\right)G' \tag{7}$$

and gyroaverage this result to find

$$\langle\delta\phi\rangle \approx \phi_* J_0\left(k_\perp v_\perp/\Omega\right)e^{iQ}, \tag{8}$$

where $\phi_* \equiv \hat{\phi}e^{iG(\psi_*)}$, $Q \equiv \left(Iv_{||}\ /\ \Omega\right)G'$ and $\vec{k}_\perp \equiv \nabla G$. However, the underlying assumption made to perform expansion (7) is that, for the particles of interest, $v_{||}$ is small. In the conventional case this is justified because neoclassical response is mainly due to the trapped and barely passing particles whose $v_{||}$ is indeed small in the large aspect ratio limit. Now that we allow a strong electric

field, the poloidal motion described by (1) suggests that the trapped-passing boundary is shifted to $v_{\|} \approx -cI\phi'(\psi)/B$. In the pedestal, $cI\phi'/B$ is of order v_i while the wavelengths of interest are of order ρ_{pol} or less. Thus, the particles contributing the most to the neoclassical polarization, have $\left(Iv_{\|}/\Omega\right)G' \sim G(\psi)$, making (7) inappropriate. To address this issue we expand G around $\psi_* - Iu/\Omega$ rather than around ψ_* itself, where u accounts for the effect of $\vec{E}\times\vec{B}$ drift and is approximately equal to $-cI\phi'/B$. The explicit definition of u in terms of constants of the motion will be provided in the next section where single particle orbits are analyzed. Now, anticipating that trapped and barely passing particles still lie within a narrow vicinity of the trapped-passing boundary, we replace (7) with

$$G(\psi) \approx G\left(\psi_* - Iu/\Omega\right) + \left[I\left(v_{\|}+u\right)/\Omega - \vec{v}\times\hat{n}\cdot\nabla\psi/\Omega\right]G', \tag{9}$$

so that we can directly adopt (8) by redefining Q as

$$Q \equiv \left[I\left(v_{\|}+u\right)/\Omega\right]G' \tag{10}$$

and ϕ_* as $\hat{\phi}e^{iG\left(\psi_* - Iu/\Omega\right)}$.

Next, we transit average (3), using $\partial g/\partial\theta_* = 0$ to leading order in the banana regime, to find

$$\frac{\partial g}{\partial t} - \overline{C_{ii}^{l}\left\{g - \frac{Iv_{\|}}{\Omega}f_M\frac{Mv^2}{2T^2}\frac{\partial T}{\partial\psi}\right\}} = \frac{Ze}{T}\frac{\partial\phi_*}{\partial t}f_M\overline{J_0\left(\frac{k_\perp v_\perp}{\Omega}\right)e^{iQ}}, \tag{11}$$

where the transit average of a quantity A is defined over a full bounce (for trapped) or a complete poloidal circuit (for passing) by

$$\overline{A} \equiv \frac{\oint A\,d\theta_*/\dot{\theta}_*}{\oint d\theta_*/\dot{\theta}_*}. \tag{12}$$

We consider the collisionless limit, and set $J_0\left(k_\perp v_\perp/\Omega\right) = 1$ since we assume $B \gg B_{pol}$. With these assumptions (11) yields

$$g = \frac{Ze}{T}\phi_* f_M \overline{e^{iQ}}\,. \tag{13}$$

To relate g and δf, the perturbation of the distribution function from its equilibrium value, we write

$$\delta f \equiv f - f_0 = f_M + g - f_0 \approx -\frac{Ze\delta\phi}{T} f_M + g\,, \tag{14}$$

where we used that $f_0 = f_M\left(\phi = \phi_0\right)$ and Taylor expanded f_M for small $\delta\phi$. Then, we obtain the linearized neoclassical relation between the density and potential response on a flux surface in a form similar to the one found in Ref.[11]:

$$\delta n = \frac{Ze}{T}\delta\phi\left\langle \int d^3v f_0 \left(e^{-iQ}\overline{e^{iQ}} - 1\right)\right\rangle_\theta, \tag{15}$$

where $\left\langle ...\right\rangle_\theta$ stands for the flux surface average. Again using that parallel velocities of the particles of interest are localized around $-u$, we expand the right side of (15) up to the second order in Q to obtain

$$\delta n = \frac{Ze}{T}\delta\phi\left\langle \int d^3v f_0 \left(i\overline{Q} - iQ - \frac{Q^2 - 2Q\overline{Q} + \overline{Q^2}}{2}\right)\right\rangle_\theta. \tag{16}$$

In the Rosenbluth-Hinton case[6], the terms of the first order in Q do not contribute to the density perturbation. Indeed, in the absence of the electric field $\overline{v}_{||}$ and $\overline{Q}$ are odd functions of $v_{||}$ while f_0 is even in it. That is, for each particle passing clockwise there is a particle with the same absolute value of $\overline{v}_{||}$ passing counterclockwise so that their cumulative response is canceled. Also, for any trapped particle $\overline{v}_{||} = 0 = \overline{Q}$. Thus, in the Rosenbluth-Hinton limit, it is the terms quadratic in Q that give the leading order response.

In our case, there is a preferred direction of rotation in the poloidal plane due to the $\vec{E}\times\vec{B}$ drift. Therefore, $\overline{Q}$ is no longer an odd function of $v_{\|}$. Neither have we $\overline{v}_{\|}=0$ for trapped particles. Thus, the terms linear in Q are expected to contribute to the neoclassical polarization. Interestingly, these terms have a preceding factor of i making the plasma susceptibility complex. Consequently, in contrast to the Rosenbluth-Hinton case there is now a spatial phase shift between the density and potential perturbations.

Once we explicitly relate δn and $\delta\phi$ with the help of (16) we are able to predict the long-term behavior of the zonal flow using the Rosenbluth-Hinton framework. Namely, we will assume that at times greater than the cyclotron period, but less than the bounce period, the potential response to the zonal flow density is solely provided by the classical polarization ε_{cl}^{pol}, whereas at the times much greater than the bounce period neoclassical shielding enters as well so that $\varepsilon^{pol}\left(t\to\infty\right)=\varepsilon_{nc}^{pol}+\varepsilon_{cl}^{pol}$. Thus, solving for the potential response to a constant density step, $\delta n\left(t\right)=\delta n\left(t=0\right)$, we obtain

$$\frac{\delta\phi\left(t\to\infty\right)}{\delta\phi\left(t=0\right)}=\frac{\varepsilon_{cl}^{pol}}{\varepsilon_{nc}^{pol}+\varepsilon_{cl}^{pol}} \tag{17}$$

with $\varepsilon_{cl}^{pol}=\omega_{pi}^{2}\,/\,\omega_{ci}^{2}$, where ω_{pi} and ω_{ci} are the plasma and ion cyclotron frequencies respectively. Notice, that in our case ε_{nc}^{pol} is complex and therefore the zonal flow residual is phase shifted with respect to the initial perturbation of the potential. In the following section, finite $\vec{E}\times\vec{B}$ drift departures from flux surfaces will be shown to substantially modify the Rosenbluth-Hinton[6] result further.

III. PARTICLE ORBITS IN A TOKAMAK PEDESTAL

In this section we analyze single ion motion in a tokamak in the presence of a strong electrostatic field. Namely, we investigate how accounting for the $\vec{E}\times\vec{B}$ drift on the right side of (1) modifies poloidal dynamics of an ion. It is necessary to emphasize that the $\vec{E}\times\vec{B}$ drift itself need not be comparable to $v_{\|}$ in order to have significant effect. In fact, due to geometrical factors even v_E of order $\left(\rho\,/\,\rho_{pol}\right)v_i \ll v_{\|}$ causes qualitative changes. Indeed, for $\rho/\rho_{pol}\ll 1$, $\vec{v}_{\|}$ is nearly perpendicular to the poloidal plane, while $\vec{v}_E$ is almost parallel to it as shown in Fig. 1. Consequently, if $|Ze\nabla\phi/T|\sim 1/\rho_{pol}$ these two streaming contributions in (1) compete in the poloidal cross-section of a tokamak.

As mentioned in the previous section, in the presence of an electric field, the trapped and barely pasing particles are spatially localized around the flux surface $\psi=\psi_*-\Delta\left(\psi_*,E,\mu\right)$ rather than around $\psi=\psi_*$ as in the conventional case. Assuming that the radial extent of particle orbits is much less than ρ_{pol}, we can Taylor expand the equilibrium electric potential around this point

$$\phi_0\approx\phi\left(\psi_*-\Delta\right)+\left[\psi-\left(\psi_*-\Delta\right)\right]\phi_0'\left(\psi_*-\Delta\right)+\frac{1}{2}\left[\psi-\left(\psi_*-\Delta\right)\right]^2\phi_0''\left(\psi_*-\Delta\right)+\ldots \quad (18)$$

Notice, that we anticipate the yet unknown parameter $\Delta\left(\psi_*,E,\mu\right)$ to be of order Iv_{th}/Ω and for this reason it would be incorrect to Taylor expand the potential around ψ_* to retain finite drift departures from a flux surface. We assume further that the radial variation of B is weak so that $B(\psi,\theta)\approx B\left(\psi_*-\Delta,\theta\right)\approx B\left(\psi_*,\theta\right)$. Then, denoting

$$\phi_*\equiv\phi\left(\psi_*-\Delta\right),\phi_*'\equiv\phi'\left(\psi_*-\Delta\right),\phi_*''\equiv\phi''\left(\psi_*-\Delta\right) \quad (19)$$

we can rewrite (1) as

$$qR_0\dot{\theta} = \left(1 + \frac{cI^2\phi_*''}{B\Omega}\right)v_{\|} + \frac{cI\phi_*'}{B} + \frac{cI\Delta\phi_*''}{B}, \tag{20}$$

where R_0 stands for the major radius and finite orbit effects are retained. Defining

$$u \equiv cI\phi_*'/B_0 \tag{21}$$

and setting $\Delta \equiv Iu/\Omega$, (20) becomes

$$qR_0\dot{\theta} = S\left(v_{\|} + u\right), \tag{22}$$

where $S \equiv 1 + cI^2\phi_*''/B\Omega$ is the orbit squeezing factor [18]. Next, we use an aspect ratio expansion to write

$$B = B_0(1+\varepsilon)/(1+\varepsilon\cos\theta) \approx B_0\left(1 + 2\varepsilon\sin^2\frac{\theta}{2}\right) \tag{23}$$

with $B_0 \equiv B(\theta = 0)$ and $\theta = 0$ at the outer equatorial plane. We also define $v_{\|0} \equiv v_{\|}(\theta = 0)$, $u_0 \equiv u(\theta = 0)$ and $S_0 \equiv 1 + cI^2\phi_*''/B_0\Omega_0$ so that $qR_0\dot{\theta}\big|_{\theta=0} = S_0\left(u_0 + v_{\|0}\right)$.

Next, we employ energy conservation

$$E \equiv \frac{v_{\|}^2}{2} + \mu B + \frac{Ze}{M}\phi(\psi) = const. \tag{24}$$

Using ψ_* conservation this becomes

$$\frac{\left(v_{\|} + u\right)^2}{2S} + \mu B - \frac{Su^2}{2} = E - \frac{Ze}{M}\left(\phi_* + \phi_*'\Delta + \frac{\phi_*''\Delta^2}{2}\right), \tag{25}$$

where all terms on the right side are constant along a trajectory. As a result, we can describe the particle motion solely in terms of θ and $\dot{\theta}$:

$$\frac{\left(q_0R_0\dot{\theta}\right)^2}{2S} + \mu B - \frac{Su^2}{2} = \frac{\left(q_0R_0\dot{\theta}_0\right)^2}{2S_0} + \mu B_0 - \frac{S_0u_0^2}{2}. \tag{26}$$

Evaluating the θ dependence of u and S with the help of (23) and solving (26) for $\dot{\theta}$ we obtain

$$\dot{\theta} q_0 R_0 = \pm \dot{\theta}_0 q_0 R_0 \sqrt{1 - \kappa^2 \sin^2\left(\theta/2\right)}, \tag{27}$$

where we assume $4\varepsilon\left(S_0 - 1\right) / S_0 \ll 1$ and define

$$\kappa^2 \equiv 4\varepsilon S_0 \frac{u_0^2 + \mu B_0}{\left(\dot{\theta}_0 q R\right)^2} = \frac{4\varepsilon}{S_0} \frac{u_0^2 + \mu B_0}{\left(u_0 + v_{||0}\right)^2} \tag{28}$$

with the trapped particles corresponding to $\kappa > 1$ and the passing to $0 < \kappa < 1$, and where $\mu B_0 \equiv v_{\perp 0}^2 / 2$. For $4\varepsilon / S_0 \ll 1$ the particles of interest are indeed localized around the trapped-passing boundary justifying our initial assumption.

It is instructive to plot the trapped-passing boundary on the $\left(v_{\perp 0}, v_{||0}\right)$ plane as shown in Fig. 2. Compared to the conventional case there are two novelties worth mentioning. First, due to the effective poloidal potential well, particles with no magnetic moment can be trapped. Second, as anticipated, the trapped particle region is no longer centered at $v_{||0} = 0$, which is the Maxwellian distribution axis of symmetry. Consequently, the terms linear in Q on the right side of (16) no longer vanish. Furthermore, for $4\varepsilon / S_0 < 1$, as u_0 grows the overlap between the trapped region and the distribution function decreases exponentially. Thus, we expect neoclassical phenomena to disappear for a strong enough electric field!

The important qualitative change in the $\left(v_{\perp 0}, v_{||0}\right)$ plane is due to the large electric field, rather than its shear. Indeed, for $u_0 = 0$ and $S_0 \gg 1$ the trapped particle region is still a cone centered at the origin[17] and therefore electric field shear alone can only modify the Rosenbluth-Hinton result algebraically. Therefore, even though S_0 is expected to contribute to neoclassical polarization, the key features in the pedestal zonal flow behavior are governed by the parameter u_0.

We are now in a position to revisit our localization assumption which allowed us to perform expansion (18). To do so we rewrite (27) as

$$u + v_{\|} = \pm\big(u_0 + v_{\|0}\big)\sqrt{1 - \kappa^2 \sin^2\big(\theta/2\big)} \tag{29}$$

so that following a given particle

$$\psi_* - \psi(\theta) = -Iv_{\|}/\Omega = -Iu/\Omega \pm (I/\Omega)\big(u_0 + v_{\|0}\big)\sqrt{1 - \kappa^2 \sin^2\big(\theta/2\big)}\,. \tag{30}$$

Then,

$$\big[\psi - \big(\psi_* - \Delta\big)\big] \approx \big(I/\Omega_0\big)\big(u_0 + v_{\|0}\big)\sqrt{1 - \kappa^2 \sin^2\big(\theta/2\big)} \lesssim \sqrt{2\varepsilon/S_0}\,\big(Iv_{th}/\Omega_0\big), \tag{31}$$

as required, while $\psi_* - \psi(\theta) \sim Iv_{th}/\Omega_0$. Thus, expanding $\phi(\psi)$ around ψ_* is not valid, while it is valid to expand $\phi(\psi)$ around $\psi_* - \Delta$ provided ε/S_0 is small enough for higher order terms in (18) to be neglected. More specifically, we require ε/S_0 to be small so that $k_{\perp}\rho_{pol}\sqrt{2\varepsilon/S_0} \ll 1$, as well as $k_{\perp}\rho_{pol} \gtrsim 1$.

Finally, we remark that the preceding results involve the parameter u_0 which is defined in terms of ψ_*. This form of u_0 is exactly what we need to find the transit average of Q and Q^2 on the right side of (16) since ψ_* must remain constant along a particle trajectory. However, the velocity integral in the same expression is to be evaluated holding ψ fixed rather than ψ_*. Therefore, it is necessary to express u_0 in terms of ψ as well. To do so we recall (19) and (21) to find

$$u = (cI/B)\phi'\big(\psi_* - Iu/\Omega\big) = (cI/B)\phi'(\psi) - (S-1)\big(u + v_{\|}\big), \tag{32}$$

where the second term on the right side of (32) is smaller than the first one by a factor of $\sqrt{\varepsilon/S_0}$. Thus, for the flux surface average we can consider

$$u_0 \approx u\big(\psi\big) \approx \big(cI/B\big)\phi'\big(\psi\big). \tag{33}$$

The integrals in (16) are evaluated in the next section.

IV. EVALUATION OF THE NEOCLASSICAL RESPONSE

Now that we have solved for the particle trajectories we can obtain an explicit expression for the neoclassical polarization in the pedestal. To do so it is convenient to define

$$Y \equiv \frac{1}{n_0}\left\langle \int_\psi d^3v f_0 \left(i\overline{Q} - iQ - \frac{Q^2 - 2Q\overline{Q} + \overline{Q^2}}{2} \right) \right\rangle_\theta \tag{34}$$

so that the zonal flow residual is given by

$$\frac{\delta\phi\left(t \to \infty\right)}{\delta\phi\left(t = 0\right)} = \frac{k_\perp^2\rho_i^2}{k_\perp^2\rho_i^2 + Y}, \tag{35}$$

where (2), (16), and (17) are used along with $\varepsilon_{nc}^{pol} = Y\omega_{pi}^2 \,/\, \left(\omega_{ci}^2 k_\perp^2 \rho_i^2\right)$. To evaluate Y we first transit average Q and Q^2 based on the particle equations of motion, and then perform the integration over velocity space and the flux surface average on the right side of (34).

A. Transit Averages

We start by noticing that to the requisite order $\overline{Q} = \left(G'I \,/\, \Omega\right)\overline{\left(v_\parallel + u\right)}$ as well as $\overline{Q^2} = \left(G'I \,/\, \Omega\right)^2 \overline{\left(v_\parallel + u\right)^2}$. Then, for passing particles ($0 < \kappa < 1$),

$$\overline{Q} = \left(G'I \,/\, \Omega\right)\frac{\pi\left(v_{\parallel 0} + u_0\right)}{2K\left(\kappa\right)} \tag{36}$$

and

$$\overline{Q^2} = \left(G'I \,/\, \Omega\right)^2 \left(v_{\|0} + u_0\right)^2 \frac{E\left(\kappa\right)}{K\left(\kappa\right)}, \tag{37}$$

where (29) is used and K and E are the complete elliptic integrals of the first and second kinds respectively:

$$E\left(\kappa\right) \equiv \int_0^{\pi/2} d\xi \sqrt{1 - \kappa^2 \sin^2 \xi}\,, \tag{38}$$

$$K\left(\kappa\right) \equiv \int_0^{\pi/2} \frac{d\xi}{\sqrt{1 - \kappa^2 \sin^2 \xi}}. \tag{39}$$

For trapped particles ($\kappa > 1$),

$$\overline{Q} = 0 \tag{40}$$

and

$$\overline{Q^2} = \left(G'I \,/\, \Omega\right)^2 \left(v_{\|0} + u_0\right)^2 \left[\frac{\kappa^2 E\left(1 \,/\, \kappa\right)}{K\left(1 \,/\, \kappa\right)} + 1 - \kappa^2\right]. \tag{41}$$

B. Velocity and Flux Surface Average Integrals

Equations (36) - (41) provide us with $\overline{Q}$ and $\overline{Q^2}$ in terms of $\left(v_{\|0} + u_0\right)$ and κ. Therefore, it is convenient to switch from integration over $\vec{v}$ to integration over $\left(v_{\|0} + u_0\right)$ and κ in (34). To account for the Jacobean of this transformation we use (29) to obtain

$$2\pi v_\perp dv_\perp dv_\| = \frac{\pi B S_0 \left(v_{\|0} + u_0\right)^2 d\kappa^2 d\left(v_{\|0} + u_0\right)}{2\varepsilon B_0 \sqrt{1 - \kappa^2 \sin^2\left(\theta \,/\, 2\right)}}. \tag{42}$$

Then, upon performing the flux surface average we rewrite (34) as

$$Y = \frac{\pi Q_0^2 S_0}{\varepsilon}\left(\frac{M}{2\pi T}\right)^{3/2} e^{M u_0^2 / T}\left(1 + \frac{iMu_0}{TQ_0}\right)\int d\kappa^2 \int d\left(v_{\|0} + u_0\right)\left(v_{\|0} + u_0\right)^4 e^{-MS_0\kappa^2\left(v_{\|0} + u_0\right)^2 / 4\varepsilon T}$$

$$\times\left\{\left[\frac{2}{\pi}E(\kappa)-\frac{\pi/2}{K(\kappa)}\right]_{0<\kappa<1}+\frac{2}{\pi\kappa}\left[\left(1-\kappa^2K(1/\kappa)+\kappa^2E(\kappa)\right)\right]_{\kappa>1}\right\}, \tag{43}$$

where $Q_0 \equiv IG'/\Omega_0$. In equation (43), the first term in the curly brackets is employed for the evaluation of the passing particle response by integrating over $0<\kappa<1$ after performing the $v_{\|0}+u_0$ integration from $\left(2/\kappa\right)\left(\varepsilon/S_0\right)^{1/2}$ to $+\infty$ and from $-\infty$ to $-\left(2/\kappa\right)\left(\varepsilon/S_0\right)^{1/2}$ (see Fig 2). The second term is used for the integration over the trapped particle region $\kappa>1$ and again between $\pm\left(2/\kappa\right)\left(\varepsilon/S_0\right)^{1/2}$ and $\pm\infty$. Letting $y=MS_0\kappa^2\left(v_{\|0}+u_0\right)^2/4\varepsilon T-Mu_0^2/T$ and replacing κ with $1/\kappa$ in the $1<\kappa$ range, the trapped particle response on the right side of (43) can be evaluated explicitly to obtain

$$Y=\frac{4}{\sqrt{\pi}}\left(\frac{q}{\varepsilon}\right)^2k_\perp^2\rho_i^2\left(\frac{2\varepsilon}{S_0}\right)^{3/2}e^{-Mu_0^2/T}\left(1+\frac{iMu_0}{TQ_0}\right)$$

$$\times\left\{\frac{4}{9\pi}+\int_0^1\frac{d\kappa}{\kappa^4}\left[\frac{2E(\kappa)}{\pi}-\frac{\pi}{2K(\kappa)}\right]\right\}\int_0^\infty dye^{-y}\left(y+\frac{Mu_0^2}{T}\right)^{3/2}, \tag{44}$$

where numerical evaluation of the expression in the curly brackets gives an approximate value of 0.193. Absent the electric field, $u_0=0$ and $S_0=1$ so that the last integral in (44) is equal to $3\sqrt{\pi}/4$ and (44) recovers the Rosenbluth-Hinton result[6]

$$Y_{RH}\approx 1.6k_\perp^2\rho_i^2\left(\frac{q}{\varepsilon}\right)^2\varepsilon^{3/2}. \tag{45}$$

Therefore, normalizing (44) to Y_{RH} we obtain the final answer in a more compact form

$$\frac{Y}{Y_{RH}}=\left(1+2i\frac{u_0/v_i}{k_\perp\rho_{pol}}\right)\frac{4e^{-\left(u_0/v_i\right)^2}}{3\sqrt{\pi}S_0^{3/2}}\int_0^\infty dye^{-y}\left[y+2\left(u_0/v_i\right)^2\right]^{3/2}. \tag{46}$$

Expression (46) possesses the features qualitatively expected. In particular, it captures a spatial phase shift between density and potential perturbations and orbit squeezing, as well as exponential decay in the large electric field limit. As anticipated, the major changes are due to the parameter u_0

rather than S_0 which only modifies the Rosenbluth-Hinton result by a factor of $S_0^{3/2}$. Notice, that for the wavelengths of order pedestal size the imaginary part of the residual is comparable to its real part and therefore simulations should reveal a non-trivial phase shift between the initial and resulting zonal flow potentials.

To see in greater detail how neoclassical polarization depends on the electric field we plot $\left|\varepsilon_{nc}^{pol}\right| / \left.\varepsilon_{nc}^{pol}\right|_{RH} = \left|Y\right| / Y_{RH}$ for $k_\perp \rho_{pol} = 1$ in Fig. 3, where $\left.\varepsilon_{nc}^{pol}\right|_{RH} \approx 1.6\left(\omega_{pi}^2 q^2\right) / \left(\omega_{ci}^2 \sqrt{\varepsilon}\right)$ is the neoclassical polarization in the tokamak core[6]. Notice that $\varepsilon_{nc}^{pol}\left(u_0\right)$ has a maximum at $u_0 \approx 1.2 v_i$. To the right of this maximum, an increase in the equilibrium electric field leads to an increase of the zonal flow residual according to (35). Recalling that in a subsonic pedestal pressure balance yields the radial Boltzmann relation between the equilibrium potential and plasma density[15],

$$d\phi_0 / d\psi \approx -\left(T / en_0\right) dn_0 / d\psi , \tag{47}$$

we find that, for a steep enough density profile, its further sharpening leads to the enhancement of the zonal flow residual. This feature has an important consequence as noted in the next section.

V. DISCUSSION AND CONCLUSION

In the preceding section we present an explicit evaluation of the collisionless neoclassical polarization and zonal flow residual in the pedestal. It importantly generalizes the classic Rosenbluth-Hinton result[6] because it allows for the strong electric field that is an intrinsic feature of a subsonic pedestal in a banana regime. The mechanism by which strong radial electric field modifies the zonal flow in the banana regime can be schematically explained in the following way.

In a pedestal of width ρ_{pol}, the electrostatic potential satisfies $|Ze\nabla\phi/T| \sim 1/\rho_{pol}$ to sustain pressure balance. A simple estimate then gives that the $\vec{E}\times\vec{B}$ drift significantly contributes to the poloidal motion of an ion, thereby qualitatively changing ion orbits compared to those in the core. Consequently, the neoclassical response to a density perturbation provided by these changed orbits modifies the Rosenbluth-Hinton zonal flow dynamics and the residual.

As it can be seen from (46), the zonal flow is sensitive to both, the absolute value of the electric field and its shear, with the former entering through the parameter u_0 and the latter through the orbit squeezing factor S_0. However, in the absence of u_0, orbit squeezing only modifies the Rosenbluth-Hinton results algebraically leaving the underlying physics otherwise unchanged. More interestingly, the electric field without shear makes the neoclassical polarization complex, resulting in a zonal flow residual that is phase shifted with respect to the initial perturbation. Moreover, for $u_0 > 1$ the neoclassical polarization decays exponentially as the square of the electric field so that the zonal flow is no longer neoclassically shielded! In this limit, the zonal flow residual approaches unity so once it is generated it can continue to act strongly in regulating the turbulent transport.

If we now imagine that zonal flow is the dominant factor limiting turbulent transport in the tokamak edge, the preceding results suggest that a strong background electric field reduces transport. This in turn suggests a feedback mechanism that could play a role in pedestal formation. Indeed, consider a tokamak with a shallow density profile and initial zonal flow. Assume that a perturbation causes a sharp density gradient. We might expect this gradient to be eliminated by transport processes. However, when the flow is subsonic, creating such a density step at the same time increases the radial electric field to sustain pressure balance (47). When this field becomes large enough for u_0 to go beyond the maximum of the curve in Fig 3 it enhances the zonal flow residual in that region

making the turbulent transport level lower and sharpening the density profile further. Thus, this feedback phenomenon may allow creation of a steep density profile before it can be relaxed by anomalous transport and therefore it could be involved in establishing, as well as maintaining, a tokamak pedestal. Importantly, it is the strength of the electric field, rather than its shear, that is expected to play the key role since it enters exponentially.

ACKNOWLEDGMENT

The authors would like to thank Felix Parra of MIT for fruitful discussions.

This research was supported by the US Department of Energy Grant No DE-FG02-91ER-54109 at the Plasma Science and Fusion Center of the Massachusetts Institute of Technology.

REFERENCES

1 P. Diamond, S. Itoh, K. Itoh and T. Hahm, Plasma Phys.Control.Fusion 47, 35–161 (2005).

2 W. Dorland, G. Hammett, Physics of Fuids B Plasma Physics 5, 812 (1993).

3 J. Candy, R. Waltz, Phys. Rev. Lett. 91, 45001 (2003).

4 Z. Lin, T. Hahm, W. Lee, W. Tang and R. White, Science 281, 1835 (1998).

5 D.R. Ernst, P.T. Bonoli, P.J. Catto, et al., Phys Plasmas 11, 2637 (2004).

6 M.N. Rosenbluth, F.L. Hinton, Phys. Rev. Lett. 80, 724 (1998).

7 F.L. Hinton, M.N. Rosenbluth, (1999).

8 Y. Xiao, P.J. Catto and K. Molvig, Phys Plasmas 14, 032302 (2007).

9 Y. Xiao, P.J. Catto, Phys Plasmas 13, 082307 (2006).

10 Belli E., Ph.D. thesis, Ph.D. dissertation, Princeton University, 2006.

11 Y. Xiao, P.J. Catto, Phys Plasmas 13, 102311 (2006).

12 F. Jenko, W. Dorland, M. Kotschenreuther and B. Rogers, Phys Plasmas 7, 1904 (2000).

13 F. Wagner, G. Becker, K. Behringer, et al., Phys. Rev. Lett. 49, 1408 (1982).

14 K. Burrell, Phys Plasmas 4, 1499 (1997).

15 G. Kagan, P.J. Catto, Plasma Phys. Controlled Fusion 50, 085010 (2008).

16 J. deGrassie, Private Communication (2008).

17 K. Shaing, R. Hazeltine, Physics of Fluids B: Plasma Physics 4, 2547 (1992).

18 R. Hazeltine, Physics of Fluids B: Plasma Physics 1, 2031 (1989).

19 H. Baek, S. Ku and C. Chang, Phys Plasmas 13, 012503 (2006).

20 McDermott et al., Bull. Am. Phys. Soc. 52, 213 (2007).

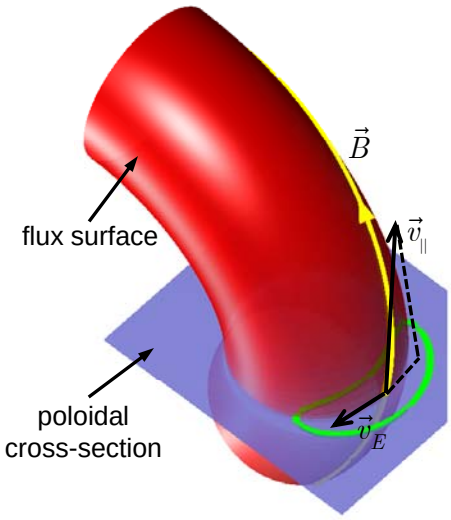

FIG. 1. Gyrocenter motion on a torus with poloidal orbit projection plotted (in green). Even though $v_{||}$ is much greater than v_E , their contributions to the poloidal motion are comparable due to geometrical effects.

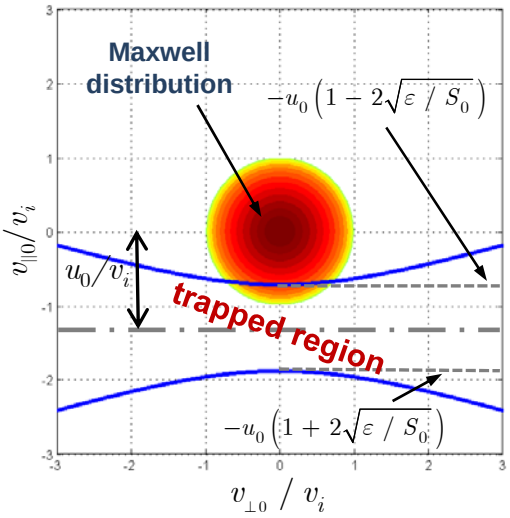

FIG. 2. The trapped particle region is shifted by a factor of u_0, while its width scales like $(\varepsilon/S_0)^{1/2}$. For $4\varepsilon/S_0<1$, as u_0 grows, the trapped particle fraction decays exponentially.

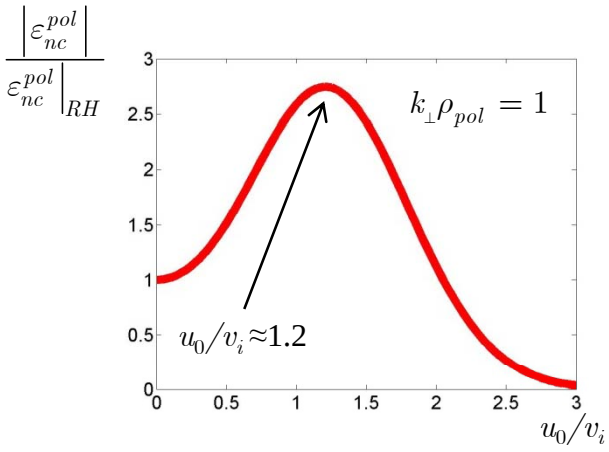

FIG. 3. Neoclassical polarization normalized to the Rosenbluth-Hinton result as a function of the equilibrium electric field.